GEOPHYSICS, VOL. 61, NO. 5 (SEPTEMBER-OCTOBER 1996): P. 1511–1523, 18 FIGS.

Velocity and interface depth determination by tomography of depth migrated gathers

Dan Kosloff*, John Sherwood‡, Zvi Koren**, Elana Machet**, and Yael Falkovitz**

ABSTRACT

A method for velocity and interface depth determination based on tomography of migrated common reflecting point (CRP) gathers is presented. The method is derived from the tomographic principle that relates traveltime change along a given ray to perturbations in slowness and layer depths. The tomographic principle is used to convert depth errors in migrated CRP gathers to time errors along a CRP ray pair and thus enable use of conventional traveltime tomography. It is also used to affect a very fast prestack migration and set up the tomography matrix. The velocity-depth determination method uses the available offsets of all CRPs and inverts for the parameters of all layers simultaneously. Hand picking of depth errors on CRP gathers is avoided by a method where the tomography matrix operates directly on the migrated gathers.

The velocity-depth determination method is demonstrated on a synthetic example and on a field example from the North Sea.

INTRODUCTION

Recent advances in depth migration have improved subsurface model construction based on reflection seismology. When no serious velocity problems exist, such as in subsalt imaging in the Gulf of Mexico, a good subsurface model can be obtained after a few iterations of depth migration followed by a redefinition of interface boundaries. However, subsurface imaging is linked to velocity, and an acceptable subsurface image can be obtained only with prior knowledge of the velocities. A good velocity determination strategy therefore becomes very important.

It has been recognized that prestack migration by itself is a most powerful velocity determination tool (Al Yahya, 1989; Faye and Jeannot, 1986). This quality is added to the ability of prestack migration to yield better results than poststack migration in complicated structures. The basic assumption underlying velocity determination methods based on prestack migration is that when the velocity is correct, all migrations with data from different domains (e.g., different offsets, different shots, different angles, etc.) must yield the same subsurface image. Conversely, when the velocity is not correct, the difference between the images can be used to improve the existing subsurface model.

The most straightforward approach in using migration is to perform analysis at selected common reflecting point (CRP) locations and use layer stripping. To determine the velocity in a layer, a suite of prestack migrations is carried out, each using a different velocity for the layer. The determined layer velocity is the one that yields the flattest CRP gather. The other methods cited use approximate theoretical results in an attempt to arrive at the correct velocity without having to perform numerous prestack migrations.

All the methods mentioned suffer from serious deficiencies. First, as with layer stripping approaches, errors in determining the velocity and interface position in the shallow layers tend to accumulate and adversely affect results in the deeper layers. Second, the CRP gathers at points different from the ones where the velocity determination was performed are often not flat. Third, when many stations are used in the analysis (perhaps to overcome the previous difficulty) the resulting velocities often turn out highly oscillatory in the lateral direction. This is caused by the nonuniqueness in the velocity-depth determination problem. With a lack of constraints, different solutions that yield flat CRP gathers can appear in the inversion. Some of these solutions may be oscillatory and physically nonsensible.

Manuscript received by the Editor November 2, 1994; revised manuscript received December 4, 1995.
*Department of Geophysics, Tel Aviv University, Tel Aviv, Israel 69978 and Paradigm Geophysical Ltd., Beit Merkazim, P.O. Box 2061, Herzlia, Israel.
‡Geophysical Development Corporation, 8401 Westheimer, Suite 150, Houston, TX 77063.
**Paradigm Geophysical Ltd., Beit Merkazim, P.O. Box 2061, Herzlia, Israel.

This paper describes an alternate approach to velocity determination based on tomography of depth migrated gathers. The idea of using this type of tomography first appeared in Stork (1992). Our approach differs from his in the spatial discretization of the subsurface and in use of a method that avoids picking depth errors on CRP gathers.

In this study, we represent the subsurface by a number of layers separated by horizons over which the velocity can change discontinuously. The input for the inversion are 2-D prestack depth migrated variable offset CRP gathers. The tomography updates slowness and layer depth changes from an initial model. For numerical reasons instead of slowness and layer depth, the actual variables used in the solution are slowness and vertical time, or layer thickness and vertical time. The slowness change allowed in a layer is vertically uniform and laterally variable in a smooth manner. The vertical time changes also vary laterally. The approach uses all the migrated gathers at once as opposed to analysis at single stations. The parameter changes of all the layers are solved for simultaneously and not by layer stripping.

The following sections describe the theory behind our depth-velocity determination method and the sequence of steps of the analysis. The method is demonstrated next with a synthetic example as well as with a field data example from the North Sea.

TOMOGRAPHIC PRINCIPLE

Consider a 2-D subsurface model consisting of a number of layers separated by reflecting horizons. We examine the ray-path of a reflected event from the N_L^{th} horizon. The traveltime along the ray is given by the integral

$$t = \int_{ray} S_L \, d\ell,$$

with $S_L(x, z)$ the medium slowness. Next consider small perturbations $(\delta S_L, \delta z_i)$ in the slowness and vertical coordinates of the intersection points of the ray with the interfaces respectively. To first order, the resulting change in traveltime is given by Farra and Madariaga (1988)

$$\delta t = \int_{ray} \delta S_L \, d\ell + \sum_{i=1}^{2N_L-1} \Delta P_z^i \delta z_i, \qquad (1)$$

ΔP_z^i is the change in the vertical slowness of the ray between points directly above and below the ith interface.

The first term on the right-hand side of equation (1) also appears in conventional cell-based tomography. The second term is more subtle and represents the traveltime change resulting from movement of interfaces that changes the length of the traversed path in each of the layers.

Equation (1) is used in this study in three important applications, conversion of migration depth errors to time errors along CRP rays, a fast prestack migration method yielding output in windows centered about the reflecting horizons, and the calculation of the tomography matrix. The following sections describe these applications in detail.

CONVERSION OF DEPTH ERRORS TO TRAVEL TIME CHANGES

This section shows how depth errors on migrated CRP gathers can be converted to time errors along CRP rays. Consider a ray pair emerging from a CRP as shown in Figure 1. The ray pair obeys Snell's law at point A. When point A is displaced vertically by an amount δz, the resulting change in traveltime can be calculated approximately using equation (1) as

$$\delta t = \Delta P_z \delta z, \qquad (2)$$

where

$$\Delta P_z = (\cos\theta_1 + \cos\theta_2)/c,$$

with c the velocity above the interface and θ_i $i = 1, 2$ is the angle of the incident or emergent ray with respect to the vertical (Figure 2). If the depth change δz is scaled to time units $\delta\tau$ according to

$$\delta z = c\frac{\delta\tau}{2}, \qquad (3)$$

then

$$\delta t = \frac{\cos\theta_1 + \cos\theta_2}{2}\delta\tau. \qquad (4)$$

This equation relates δt and $\delta\tau$ by a stretch factor.

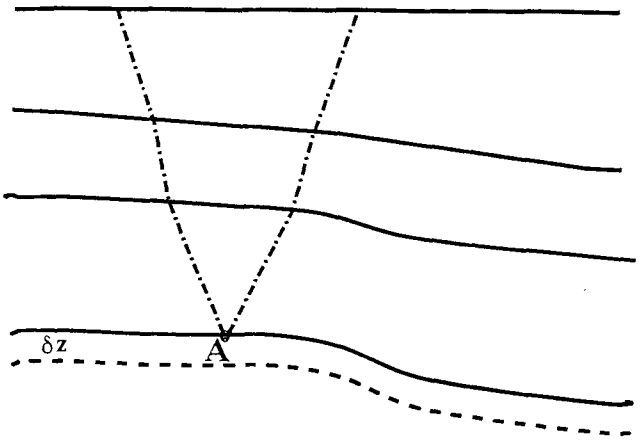

FIG. 1. Conversion of depth errors to time errors.

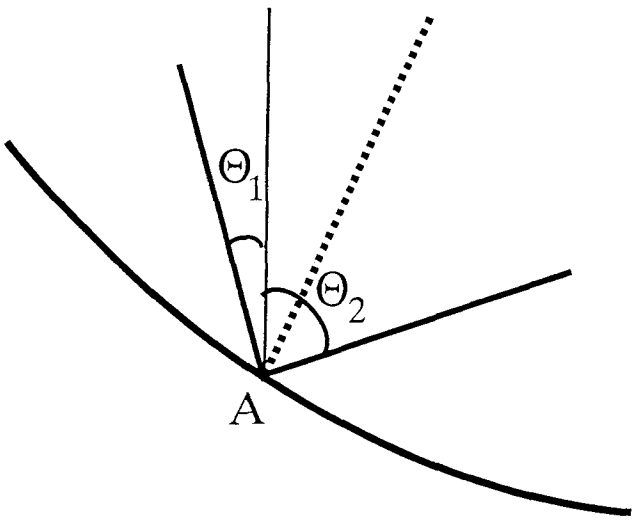

FIG. 2. Vertical slowness angles at reflection.

Here, δz can represent the difference in the depth of a layer image and a reference depth. Correspondingly, δt will be the difference between the traveltime along a CRP ray pair to and from the reference depth and the traveltime to and from the layer image. Equations (3) and (4) thus convert depth errors to time errors along the CRP ray pair. This conversion enables use of the well established time tomography on depth-migrated gathers where the input becomes δt of all CRPs, layers, and offsets instead of δz.

The tomographic equations are insensitive to constant time shifts of all the traces in the CRP gather. Therefore the reference depth is somewhat arbitrary. This study uses correlated CRP gathers where the reference depth is the depth of the center of the window of the crosscorrelation.

MODEL-BASED IMAGING

Model-based imaging is a fast prestack migration designed for velocity analysis. The output of the migration is CRP gathers in windows centered at the reflecting horizons. Approaches similar to the one described here have appeared in a patent by Johnson (1990) and in Landa and Sorin (1993).

A CRP ray pair, which emanates from a reflecting horizon and obeys Snell's law, establishes a relationship between a CRP and the midpoint of the rays on the surface (m' in Figure 3). In a true-summation common-offset migration, all shot receiver pairs with the given offset contribute to the image at the CRP. However, for a reflection event, the shot receiver pair with closest midpoint to m' (m in Figure 3) will contribute the largest amplitude to the image at the CRP. Accordingly, only this trace is used in model-based imaging. This single-trace aperture migration is basically a resort from common-midpoint (CMP) order to CRP order where the connection is established by the ray tracing. In this sort, a single CMP may contribute to a number of CRPs in different layers.

A typical time gate for the model based imaging is 100 ms. In the tomography, the results are used directly in the time domain. If, however, the results need to be converted to vertical time or to depth, the stretch factor derived in the previous section needs to be applied. When the midpoint m' differs from the nearest CMP m (Figure 3), the reflection time at m' is obtained from the time at m using a first-order correction

$$t_{m'} \approx t_m + (x_{m'} - x_m)(P_1 + P_2).$$

P_1 and P_2 are the respective ray parameters at the surface of the CRP rays.

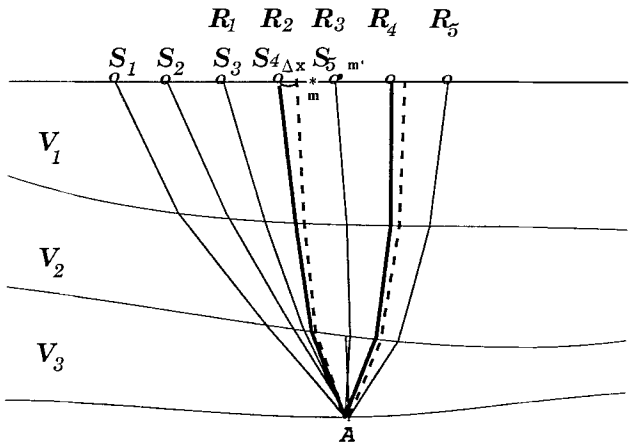

FIG. 3. CRP raypaths for common-offset migration. Left pointing arrows indicate shot positions, and right pointing arrows indicate receiver positions.

CONSTRUCTION OF THE TOMOGRAPHY MATRIX

The tomography is designed for 2-D common-offset migration for layered structures with interfaces that run clearly across the model. Pinchouts are accounted for by zero thickness layers. The velocity within a layer can be completely variable in the lateral direction and can vary linearly in the vertical direction. The velocity changes calculated by the tomography can also vary laterally but are vertically constant.

The changes in layer slowness and layer depths (or equivalently slowness and vertical time as described in the next section) are calculated at equally spaced spline nodes. The typical distance between nodes is 20–30 CMP intervals. Values of the slowness and layer depth updates at points between nodes are interpolated by a two-point Hermite interpolation. The variable derivatives for the interpolation are evaluated by central differencing. In a given interval $[x_i, x_{i+1}]$ the slowness change for the jth layer is interpolated according to

$$\delta S_L^j(x) = \phi_{-1}(x)\delta S^j_{L_{i-1}} + \phi_0(x)\delta S^j_{L_i} + \phi_1(x)\delta S^j_{L_{i+1}} + \phi_2(x)\delta S^j_{L_{i+2}}, \quad (5)$$

where $\delta S^j_{L_i}$ is the slowness update at the ith node and jth interface, and the weights $\phi_k(x)$ are given in Appendix A. A similar formula applies to the layer depth updates δz.

We denote by $\delta\mathbf{m}$ the vector of the slowness and layer depth updates at all the spline nodes. Let $\delta\mathbf{t}$ represent the time errors at all CRPs for all offsets and layers. A substitution of equation (5) and the equivalent formula for the layer depth updates into the tomographic principle equation (1) results in a relationship of the form

$$\delta\mathbf{t} = \underset{\sim}{\mathbf{A}}\delta\mathbf{m}.$$

The dimension of $\delta\mathbf{m}$ equals twice the number of spline nodes in a layer times the number of layers. For each component of $\delta\mathbf{t}$ the construction of the elements of the influence matrix $\underset{\sim}{\mathbf{A}}$ for the depth change variables involves calculation of the spline weights at the intersection points of the rays with the layers, and for the slowness change, consists of an integration of the interpolation weights along the rays.

CONVERSION TO VERTICAL TIME AND NORMALIZATION INTO TIME UNITS

We have found it advantageous to convert the parameters from slowness and depth change to slowness and vertical time change or layer thickness and vertical time change. After the conversion the parameters are scaled to time units. From tests on simple models it appears that the $\underset{\sim}{\mathbf{A}}$ matrix is better conditioned after the conversion and the normalization to time facilitates the assignment of weights in the least-squares formulation of the tomography.

With z_k denoting the depth of the kth interface at a certain CMP station, the layer thickness is given by $h_k = z_k - z_{k-1}$. Conversely, $z_k = \sum_{i=1}^{k} h_i$ and hence perturbations in layer depth are related to thickness perturbations by

$$\delta z_k = \sum_{i=1}^{k} \delta h_i. \tag{6}$$

Equation (6) is used for the conversion from layer depth parameters to thickness parameters. Such a conversion is possible in configurations where the spline nodes for all layers are at the same horizontal positions.

The vertical time is defined by

$$t_{v_k} = 2\sum_{i=1}^{k} h_i S_{L_i},$$

or recursively

$$t_{v_k} = t_{v_{k-1}} + 2h_k S_{L_k},$$

and thus

$$\delta t_{v_k} = \delta t_{v_{k-1}} + 2\delta h_k S_{L_k} + 2h_k \delta S_{L_k}.$$

We normalize slowness and thickness perturbations to time units by $\delta h'_k = \delta h_k S_{L_k}$ and $\delta S'_{L_k} = h_k \delta S_{L_k}$ to obtain

$$\delta t_k = \delta t_{k-1} + 2\delta h'_k + 2\delta S'_{L_k}.$$

This simple relationship together with equation (6) is used to convert the original parameters to slowness and vertical time change, or alternatively, to thickness and vertical time change. In most situations, we use slowness and vertical time; however, there are cases, such as the elimination of residual statics, where one may wish to fix the thickness of a certain layer and then the second set of variables is used.

WEIGHTED LEAST SQUARES

The system of equations relating time errors to parameter changes is highly over determined and is solved by weighted least squares. The resulting system is written as

$$(\underset{\sim}{\mathbf{A}}^T \underset{\sim}{\mathbf{C}}_D^{-1} \underset{\sim}{\mathbf{A}} + \underset{\sim}{\mathbf{C}}_M^{-1}) \delta\mathbf{m} = \mathbf{A}^T \underset{\sim}{\mathbf{C}}_D^{-1} \delta\mathbf{t}, \tag{7}$$

where $\underset{\sim}{\mathbf{C}}_D$ is the data covariance matrix containing the variance of the data on its diagonal, and $\underset{\sim}{\mathbf{C}}_M$ is the parameter covariance matrix. The data standard deviation is estimated according to the data quality of the horizons selected for the inversion. Typical values are one to two time samples. The parameter covariance matrix controls the sensitivity of the inversion. Typical values for the standard deviation are one time sample for the vertical time and one time sample per one second of vertical traveltime in the layer for the slowness or thickness variables. An additional small component of the $(-1, 2, -1)$ smoothing operator is added to each of the two variables in each layer to further stabilize the tomography.

To calculate the right-hand side of equation (7), one normally would need picks of δt. In this study, however, we use a procedure developed by Sherwood et al. (1986), where the right-hand side of equation (7) is calculated after the matrix $\underset{\sim}{\mathbf{A}}^T \underset{\sim}{\mathbf{C}}_D^{-1}$ operates directly on the CRP gathers. A similar approach was used by Tieman (1991). Instead of using the original gathers, we use correlated gathers where first a model trace is formed by a stack of the member traces of the gather, and then each trace is cross correlated with the model trace to form the correlated gather. Details of the procedure are given in Appendix B.

SYNTHETIC EXAMPLE

We first demonstrate the tomography with a synthetic example. The true structure consisted of three flat layers each with a thickness of 1000 m (Figure 4). The first and third layers had constant velocities of 2000 m/s and 4000 m/s, respectively. In the second layer, the velocity was 2400 m/s on one side and 3400 m/s on the other side, and in the middle there was a narrow transition zone between the two velocities. A synthetic survey was calculated for this model. The distance between CMPs was 20 m, the first offset distance was 0 m, and the maximum number of offsets was 50 with an increment of 50 m between the offsets.

Figure 5 shows the zero-offset time section that corresponds to this structure. For the example, we started with uniform velocities of 1800 m/s, 2800 m/s, and 4400 m/s for the three layers, respectively. An initial model (Figure 6) was derived by ray migrating the zero-offset time section with the assumed layer velocities. This same procedure is used with real data except when the structure is too complicated to pick on CMP stacked sections. The field example of the next section is such a case. In such situations, it is preferable to pick on time-migrated sections and then image-ray migrate or alternatively demigrate the horizons to produce input for the ray migration.

The determination of the subsurface structure was performed in four iterations. The input for each iteration consisted of a depth-velocity model and the original synthetic CMP gathers. The data was then migrated by model-based imaging to produce CRP gathers that were supplied to the tomography algorithm. The tomography then calculated an improved depth-velocity model that yielded flatter CRP panels. Our experience indicates that one needs to apply a deep mute to the data during the initial iterations and then relax the mute during the final iterations as the velocities converge to the correct values. The mute cutoff point was selected at the offset where the main portion of the wavelet comes out of the crosscorrelated gather window. Consequently in the first iteration we used 10, 13, and 18 offsets for the three layers, respectively, in the third iteration we used 25, 29, and 38 offsets, while in the final iteration we used all offsets.

Figures 7 and 8 show correlated CRP gathers to stations 100 and 400, respectively, for the initial model, and for the first, second, and fourth iteration of tomography, respectively. The figures clearly show the improvement after each additional iteration. A comparison of the resulting depth-velocity model (Figure 9) with the correct model (Figure 4) shows that the tomography was able to eliminate most of the error in the initial model. Additional iterations would have improved the model further, but beyond a certain point one reaches a point of diminishing returns. Moreover, in real data, one usually does not have the range of offsets present in this example, as even here it can be noticed that the far-offset traces of the CRP panels are contaminated by the crossover of reflections from other layers.

This example has demonstrated the ability of the tomography to resolve lateral velocity changes. The approach of using a

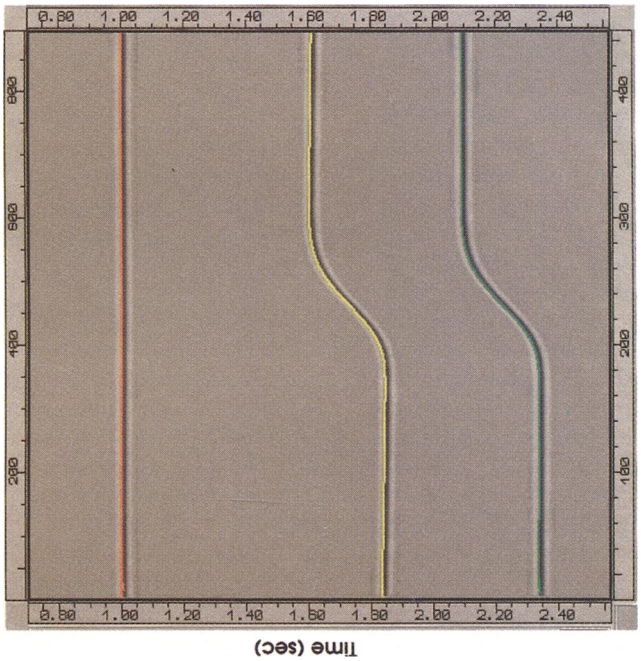

FIG. 5. Zero-offset time section for synthetic example.

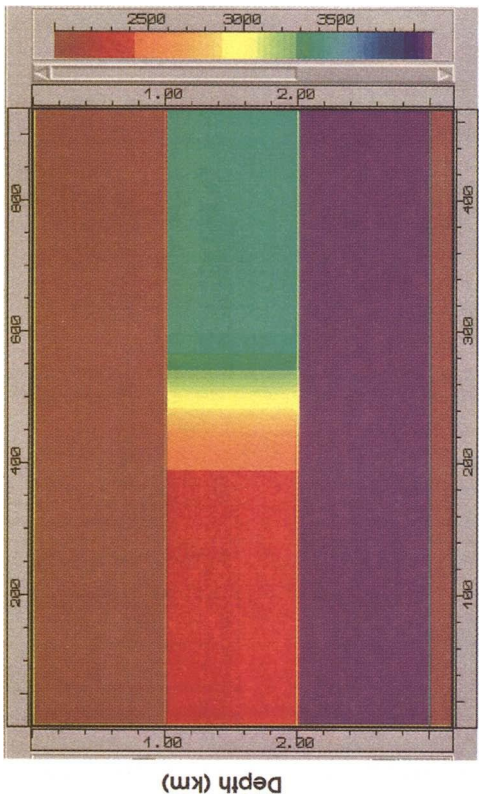

FIG. 4. True depth-velocity model for the synthetic example.

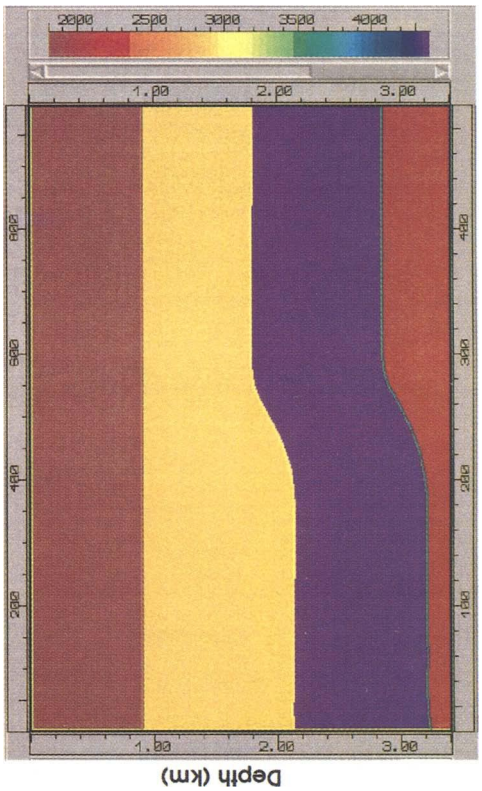

FIG. 6. Initial model from ray migration of the zero-offset time section.

few offsets in the first iterations when the errors and moveout are large and subsequently increasing the number of offsets appears to be a feasible procedure to use in general.

FIELD DATA EXAMPLE

The tomographic algorithm is tested next with a 2-D line from the North Sea. The line contained 1034 CMPs with a spacing of 25 m between stations. Based on a preliminary velocity analysis, partial normal moveout (NMO) was applied to have all CMPs with the same offsets. The number of offsets was 48 with an offset interval of 50 m. The near offset was 50 m. The data was recorded to 5 s with a sample rate of 4 ms.

The first step in the velocity determination procedure was the generation of an initial model. For this objective, prestack time migration was carried out (Figure 10). Prestack time migration yields a better image than poststack migration for this data and for other examples where CMP stacking is not completely successful. The initial model (Figure 11) was generated by picking a number of horizons of Figure 10 and image-ray migrating the horizons to produce a depth-velocity model. Layer velocities with gradients that were derived from a well (marked in Figure 11) were selected for generating the initial model by image ray migration.

Three tomography iterations were performed for obtaining an improved depth-velocity model. CRP panels before and after the tomography are shown in Figures 12 and 13. The improvement in the flatness of the panels by the tomography is apparent. The updated depth-velocity model is shown in Figure 14. This model is quite different from the initial model, and in some locations, the velocity changes were hundreds of meters per second.

After obtaining an updated depth-velocity model, prestack depth migration was carried out on the data. The migration algorithm was a Kirchhoff type where the traveltimes were obtained by the wavefront method (Vinje et al., 1993). Figures 15 and 16 show stacks of CRP gathers that were obtained after migration with the initial and final depth-velocity models, respectively. Comparison of the two sections shows the improvement brought about by the tomography. In addition, Figures 17 and 18 present unstacked migrated CRP gathers at stations 320 and 717, for the initial model and for the tomographically updated model. As the figures show, after the tomography most events on the gathers are quite flat.

CONCLUSIONS

We have described a tomographic approach for deriving a subsurface depth-velocity model from reflection seismograms. This model yields flat migrated CRP panels and represents a smoothed approximation to the real subsurface velocities. Traveltime information present in the seismic data is accounted for. However, to constrain physical parameters further, additional data like amplitudes or well information would be needed.

The inversion procedure has two major stages, first, the generation of an initial model, and second, a tomographic inversion for velocities and interface depths. It is advisable to keep the initial model as simple as possible. The approach we prefer and have used in the field example is to perform prestack time migration on the input gathers. A number of horizons on the migrated section are then selected and digitized. Image ray migration, or demigration followed by ray migration of the picked horizons is performed. The velocities for the image ray migration should be simple like the constant velocities we have used

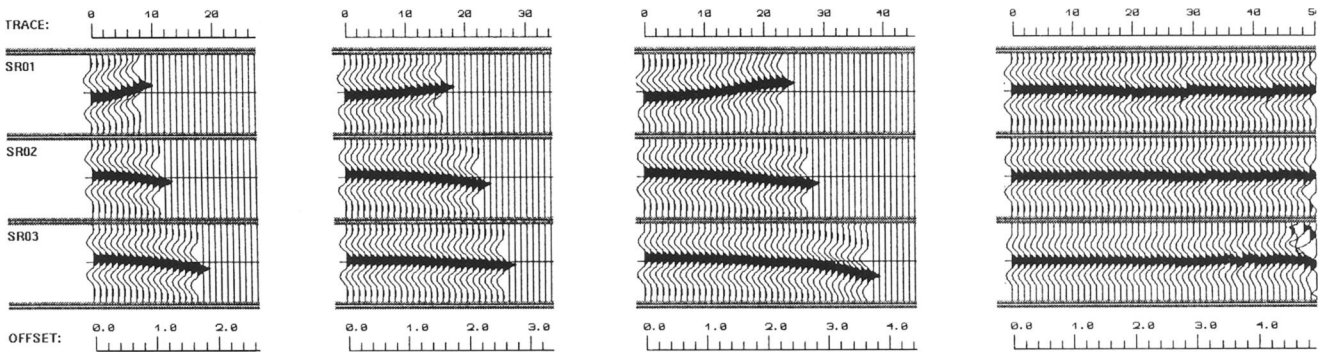

FIG. 7. CRP gathers before (left) and after (right) tomography at station 100.

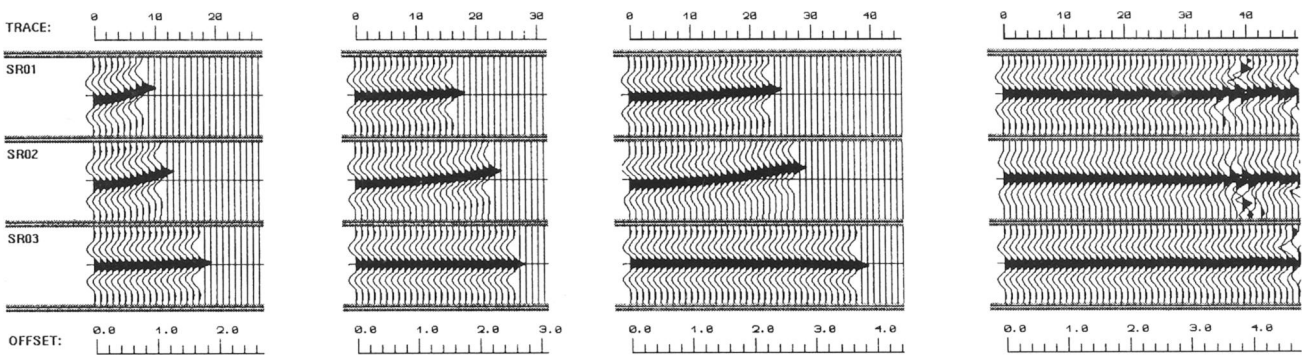

FIG. 8. CRP gathers before (left) and after (right) tomography at station 376.

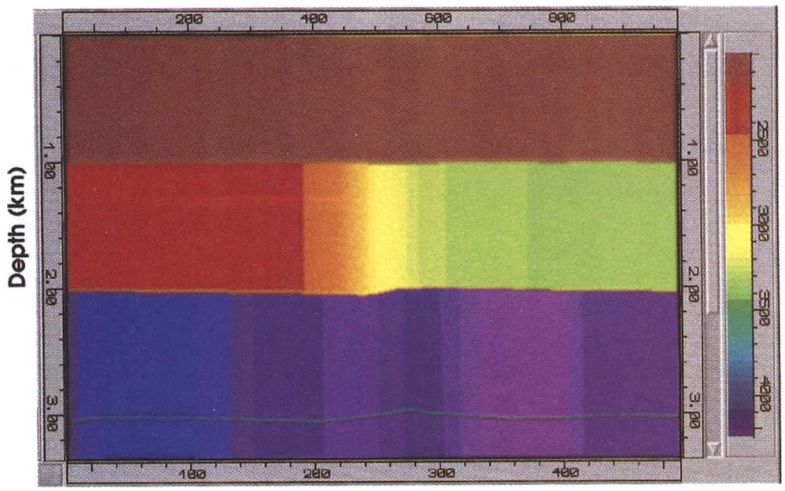

FIG. 9. Depth-velocity model for the synthetic example after four iterations of tomography.

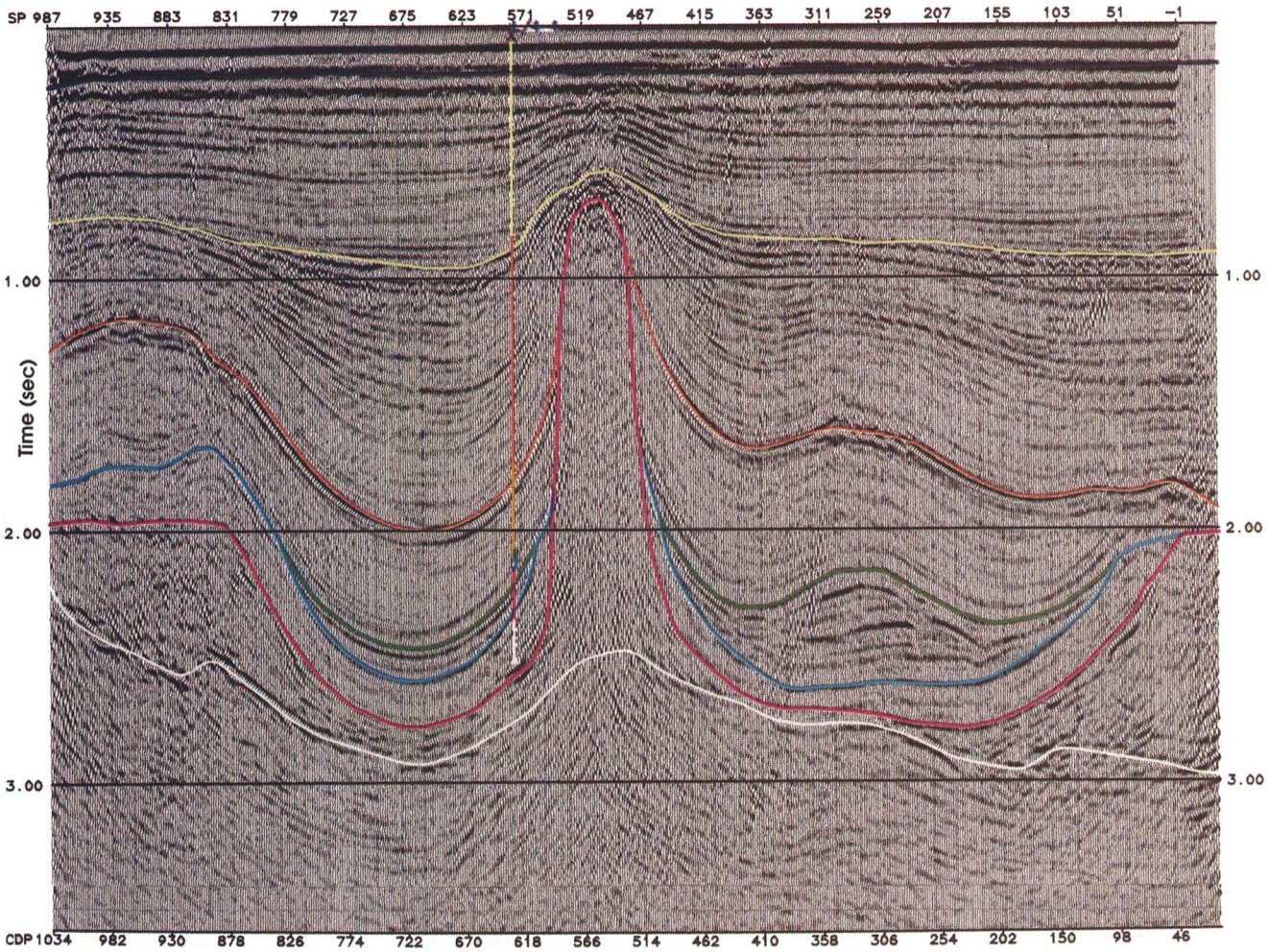

FIG. 10. Time-migrated section of North Sea data.

in the examples in this work. Attempts to use more detailed initial models can be counter-productive and lead to doubts whether the final results are genuine or merely a result of the choice of the initial model.

In practically all cases we have encountered, the tomography has been able to resolve the depth-velocity model in a few iterations. In the first iterations when the depth-velocity model is far from the correct one it is important to apply a deep mute to the data. In later iterations the mute can be relaxed. The tomographic procedure combined with the procedure for avoiding picking of events on CRP gathers requires very little user intervention. This feature will gain added importance in three dimensions where the amount of labor with some other methods can become overwhelming.

The issue of depth-velocity ambiguity is ever present with velocity inversion methods. It has been demonstrated (e.g., Bickel, 1990) that even with very simple models there is a nonuniqueness in the velocity-depth determination problem. In practical terms, this means that there can be a number of models that satisfy observations equally well and flatten CRP panels. The tomography approach tackles this issue by allowing only smooth updates of the initial model through spline interpolation. Thus for a simple initial model, the tomography will tend to give the smoothest model that satisfies the data. This may be the best alternative for lack of other information. In other situations, it may be desirable to incorporate prior knowledge into the inversion, or scan a range of initial models to evaluate the uncertainty in the output results.

ACKNOWLEDGMENT

We wish to thank Elf Aquitainne for providing the field data for testing the tomographic inversion.

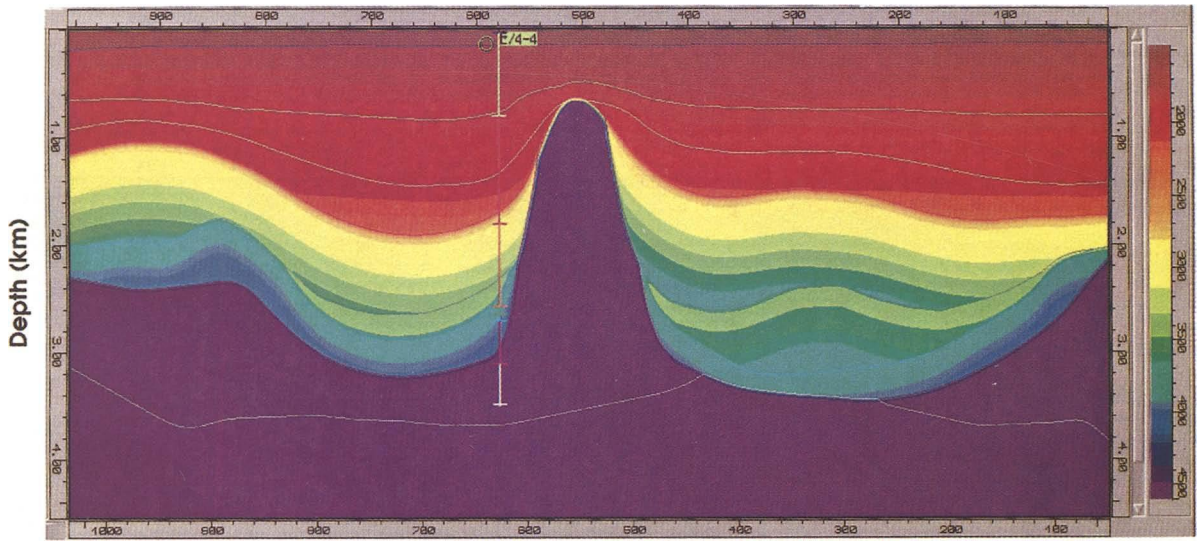

FIG. 11. Initial model for the field data example.

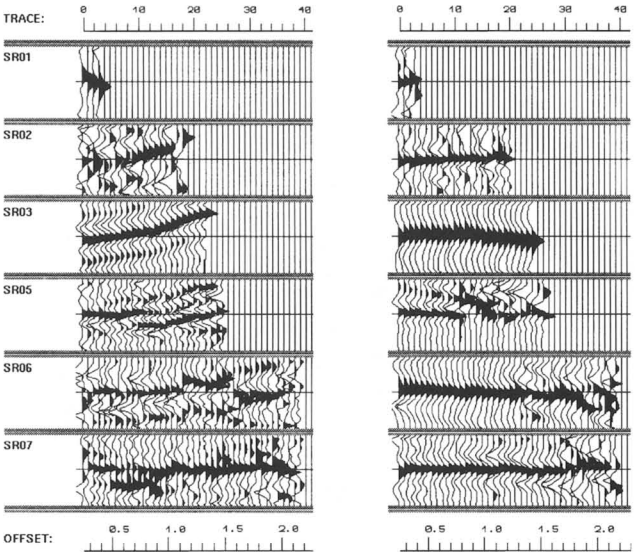

FIG. 12. CRP panels for station 320 from the initial and final models of the field data example.

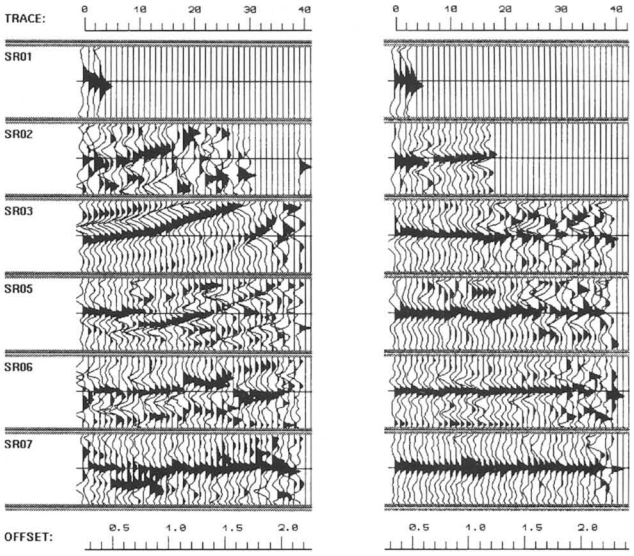

FIG. 13. CRP panels for station 717 from the initial and final models of the field data example.

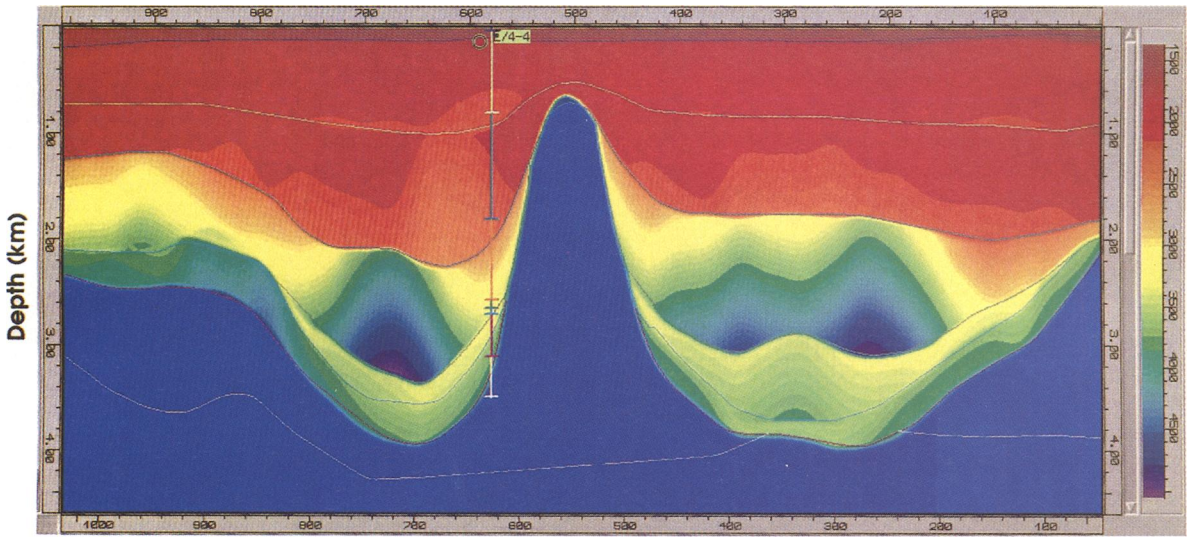

FIG. 14. Depth velocity model for the field data example after three tomography iterations.

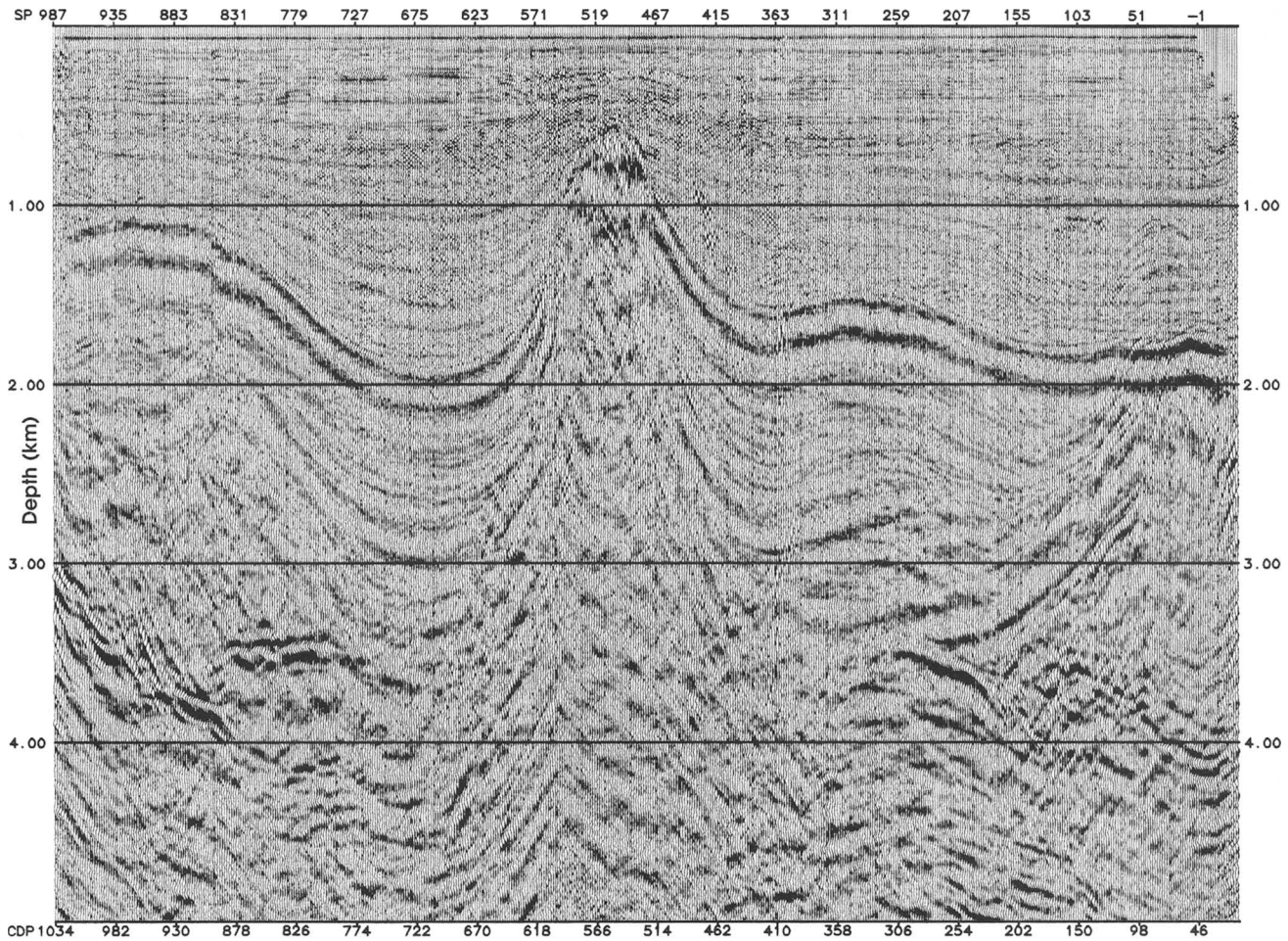

FIG. 15. Stacked depth-migrated section for the field data example using initial depth-velocity model.

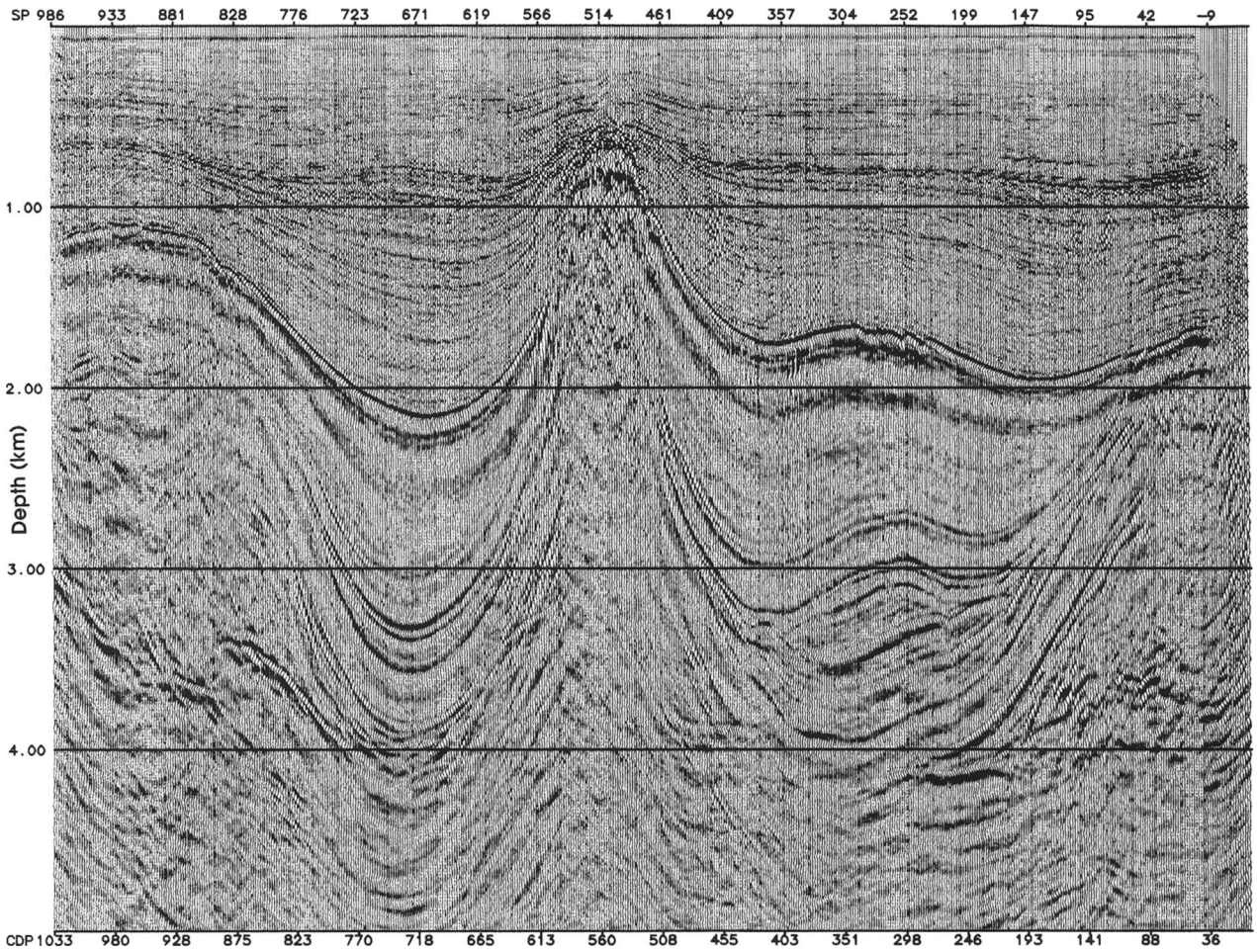

FIG. 16. Stacked depth-migrated section for the field data example using final depth-velocity model.

REFERENCES

Al Yahya, K. M., 1989, Velocity analysis by iterative profile migration: Geophysics, **54**, 718–729.
Bickel, S. H., 1990, Velocity-depth ambiguity of reflection travel times: Geophysics, **55**, 266–278.
Farra, V., and Madariaga, R., 1988, Nonlinear reflection tomography: Geophys. J. Internat., **95**, 135–147.
Faye, J. P., and Jeannot, J. P., 1986, Prestack migration velocities from focusing depth analysis: 56th Ann. Internat. Mtg.: Soc. Expl., Geophys., Expanded Abstracts, 438–442.
Johnson, C., 1990, Patent number 4,953.142, Marathon Oil Company.
Landa, E., and Sorin, V., 1993, Fast prestack migration by CRP stacking. EAEG Extended Abstracts, 120.
Ralston, A., and Rabinowitz, P., 1978, A first course in numerical analysis: McGraw-Hill Book.
Sherwood, J. W. C., Chen, K. C., and Wood, M., 1986, Depth and interval velocities from seismic reflection data for low relief structures: 18th Ann. Offshore Tech. Conf.
Stork, C., 1992, Reflection tomography for the post-migrated domain, Geophysics, **57**, 680–692.
Tieman, H. J., 1991, Migration velocity analysis through weighted stacking: 61st Ann. Internat. Mtg., Expanded Abstracts, 1243–1246.
Vinje, V., Iversen, E., and Gjoysstdal, H., 1993, Traveltime and amplitude estimation using wavefront construction. Geophysics, **58**, 1157–1166.

APPENDIX A

HERMITE SPLINE INTERPOLATION

The formula for the two-point Hermite interpolation reads (Ralston and Rabinovitch, 1978),

$$y(x) = \sum_{j=0}^{1} h_j(x) f(x_j) + \sum_{j=0}^{1} \hat{h}_j(x) f(x_j),$$

where

$$h_j(x) = (1 - 2(x - x_j)\ell_j'(x_j))\ell_j^2(x), \quad j = 0, 1,$$

and

$$\hat{h}_j(x) = (x - x_j)\ell_j^2(x), \quad j = 0, 1,$$

with

$$\ell_0(x) = \frac{x - x_1}{x_0 - x_1},$$

and

$$\ell_1(x) = \frac{x_0 - x}{x_0 - x_1}.$$

Here, $f(x_j)$ and $f'(x_j)$ are, respectively, values of the interpolated function and its derivative at the two ends of the interpolation interval, while $y(x)$ is the result of the interpolation.

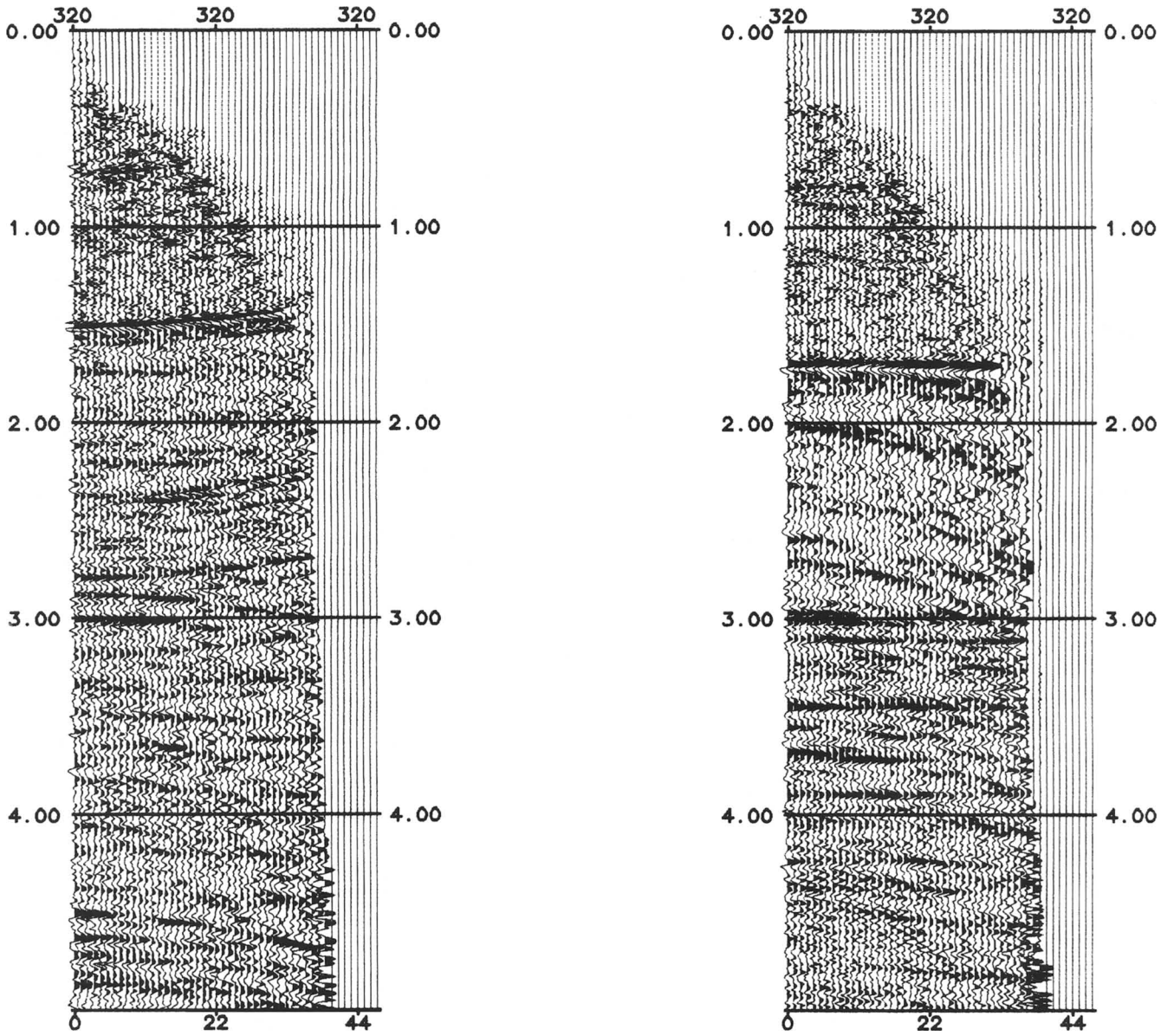

FIG. 17. Unstacked CRP gathers for station 320 for the initial and final models of the field data example.

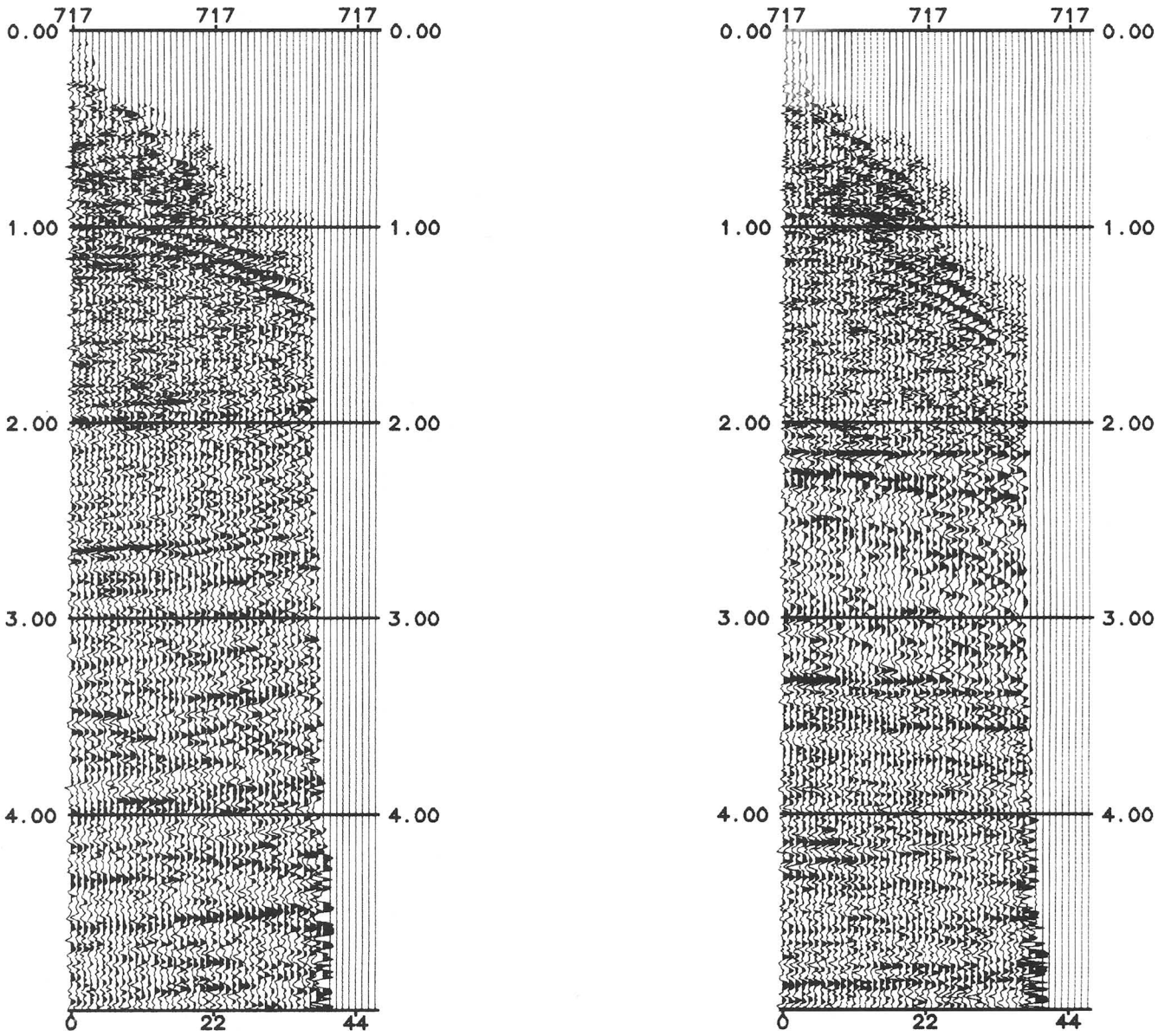

FIG. 18. Unstacked CRP gather for station 717 for the initial and final models of the field data example.

We consider uniform spacing dx between nodes and approximate the derivative of $f(x)$ by the central difference formula

$$f'(x_j) = \frac{f(x_{j+1}) - f(x_{j-1})}{2dx}.$$

After denoting $x = x_0 + \delta dx (0 \le \delta < 1)$, the Hermite spline interpolation becomes,

$$y(x) = \phi_{-1}(\delta) f(x_{-1}) + \phi_0(\delta) f(x_0) + \phi_1(\delta) f(x_1) + \phi_2(\delta) f(x_2),$$

where

$$\phi_{-1} = -\tfrac{1}{2}\delta(\delta - 1)^2,$$

$$\phi_0 = (1 + 2\delta)(\delta - 1)^2 - \tfrac{1}{2}(\delta - 1)\delta^2,$$

$$\phi_1 = (1 - 2(\delta - 1))\delta^2 + \tfrac{1}{2}\delta(\delta - 1)^2,$$

$$\phi_2 = \tfrac{1}{2}(\delta - 1)\delta^2.$$

APPENDIX B

AVOIDING PICKING

The right-hand side of equation (7) can be written as a matrix times vector product $\sum_{j=1}^{d} B_{ij}\delta t_j, i = 1, \ldots, M$, where $\underset{\sim}{\mathbf{B}} = \underset{\sim}{\mathbf{A}}^T \underset{\sim}{\mathbf{C}}_d^{-1}$. The first index of $\underset{\sim}{\mathbf{B}}$ corresponds to the model space while the second index corresponds to the data space (e.g., all offsets of all CRPs of all layers). To calculate this term, one normally would first need to pick the traveltime residuals $\delta\mathbf{t}$. This Appendix describes an alternative procedure that avoids this step.

The tomography uses correlated CRP gathers. In these gathers only a small time window around the reflections from the layers is used. Each portion of a trace within a window defines an event $f_j(t)$, where j is the event number and t varies over the time range of the window. All events are normalized to the same maximum amplitude. Furthermore, we make the assumption that they contain an identical zero phase wavelet function however they may be shifted by different time shifts δt_j. We can therefore write

$$f_j(t) = W(t - \delta t_j), \qquad -T_g/2 < t < T_g/2,$$

where $W(t)$ is the wavelet function and T_g is the size of the time gate.

By the Fourier theorem

$$f_j(t) = W(t - \delta t_j) = \frac{1}{2\pi}\int_{-\infty}^{\infty} \tilde{W}(\omega) e^{i\omega(t - \delta t_j)}\, d\omega,$$

where ω is the angular frequency and $\tilde{W}(\omega)$ is the Fourier transform of $W(t)$.

Forming the inner product of the $\underset{\sim}{\mathbf{B}}$ matrix with $\mathbf{f(t)}$ and then changing the order of integration and summation yields

$$\sum_j B_{ij} f_j(t) = \frac{1}{2\pi}\int_{-\infty}^{\infty} \tilde{W}(\omega) e^{i\omega t}\left(\sum_j B_{ij} e^{-i\omega\delta t_j}\right) d\omega.$$

For small time shifts Δt_j one obtains to first order

$$\sum_j B_{ij} e^{-i\omega\delta t_j} \approx \sum_j B_{ij}(1 - i\omega\delta t_j) = \sum_j B_{ij}\left(1 - i\omega\frac{\sum_j B_{ij}\delta t_j}{\sum_j B_{ij}}\right) \approx \sum_j B_{ij} e^{-i\omega\tau},$$

where

$$\tau = \frac{\sum_j B_{ij}\delta t_j}{\sum_j B_{ij}}.$$

Therefore,

$$\sum_j B_{ij} f_j(t) \approx \frac{1}{2\pi}\int_{-\infty}^{\infty} \tilde{W}(\omega) e^{i\omega(t-\tau)}\left(\sum_j B_{ij}\right) d\omega = \frac{1}{2\pi}\left(\sum_j B_{ij}\right) W(t - \tau).$$

The term $\sum_j B_{ij} f_j(t)$ represents a weighted stack of all events in the CRP gathers. Picking the time τ of the maximum of the stacked trace can be done on the computer in a robust manner. The left-hand side of equation (7) can be calculated approximately according to

$$\sum_j B_{ij}\delta t_j \approx \left(\sum_j B_{ij}\right)\tau.$$

Because of the linearization involved, this procedure will apply only to gathers exhibiting small delays δt_j. In practice, δt_j is limited to a few samples, and the gathers are muted at the offset where δt_j exceeds this value.